Journal of Zhejiang University SCIENCE A
ISSN 1673-565X (Print); ISSN 1862-1775 (Online)
www.zju.edu.cn/jzus; www.springerlink.com
E-mail: jzus@zju.edu.cn

Similarity-based denoising of point-sampled surfaces*

Ren-fang WANG[†1,2], Wen-zhi CHEN[1], San-yuan ZHANG[†‡1], Yin ZHANG[1], Xiu-zi YE[1]

([1]*School of Computer Science and Technology, Zhejiang University, Hangzhou 310027, China*)

([2]*Faculty of Computer Science and Information Technology, Zhejiang Wanli University, Ningbo 315100, China*)

[†]E-mail: wrfwpln@126.com; syzhang@cs.zju.edu.cn

Received Sept. 2, 2007; revision accepted Mar. 28, 2008

Abstract: A non-local denoising (NLD) algorithm for point-sampled surfaces (PSSs) is presented based on similarities, including geometry intensity and features of sample points. By using the trilateral filtering operator, the differential signal of each sample point is determined and called "geometry intensity". Based on covariance analysis, a regular grid of geometry intensity of a sample point is constructed, and the geometry-intensity similarity of two points is measured according to their grids. Based on mean shift clustering, the PSSs are clustered in terms of the local geometry-features similarity. The smoothed geometry intensity, i.e., offset distance, of the sample point is estimated according to the two similarities. Using the resulting intensity, the noise component from PSSs is finally removed by adjusting the position of each sample point along its own normal direction. Experimental results demonstrate that the algorithm is robust and can produce a more accurate denoising result while having better feature preservation.

Key words: Point-sampled surfaces (PSSs), Similarity, Geometry intensity, Geometry feature, Non-local filtering
doi:10.1631/jzus.A071465 **Document code:** A **CLC number:** TP391.7

INTRODUCTION

Point-sampled models without topological connectivity are normally generated by sampling the boundary surface of physical 3D objects with 3D-scanning devices. Despite the steady improvement in scanning accuracy, undesirable noise is inevitably introduced from various sources such as local measurements and algorithmic errors. Thus, noisy models need to be denoised or smoothed before performing any subsequent geometry processing such as simplification, reconstruction and parameterization. It remains a challenge to remove the inevitable noise while preserving the underlying surface features in computer graphics. In particular, fine features are often lost if no special treatment is provided.

In recent years, a variety of point-based denoising and smoothing approaches have been introduced, and they can be roughly categorized into the following four groups:

(1) Spectral techniques. The techniques of spectral filters in image setting were generalized to point-based surfaces, for example, Pauly and Gross (2001) created a spectral decomposition of a point cloud and denoised it by manipulation of the spectral coefficients.

(2) Interpolation or approximation approaches. The raw point clouds are interpolated or approximated with smooth surfaces such as extremal surfaces (Amenta and Kil, 2004), implicit surfaces (Carr *et al*., 2001; Samozino *et al.*, 2006; Daniels II *et al.*, 2007), moving least-squares (MLS) surfaces (Mederos *et al.*, 2003; Weyrich *et al.*, 2004; Dey and Sun, 2005; Lipman *et al.*, 2006; Daniels II *et al.*, 2007) and local parametric surfaces (Pauly *et al.*, 2003), etc.

(3) Statistical techniques. Based on robust statistics, the smoothing techniques for point-sampled surfaces (PSSs) were introduced. Pauly *et al*.(2004)

‡ Corresponding author

* Project supported by the Hi-Tech Research and Development Program (863) of China (Nos. 2007AA01Z311 and 2007AA04Z1A5), and the Research Fund for the Doctoral Program of Higher Education of China (No. 20060335114)

proposed a framework for analyzing shape uncertainty and variability in point-sampled geometry based on statistical data analysis, which can be applied to reconstruct surfaces in the presence of noise. Schall *et al.*(2005) developed a method for robust filtering of a given noisy point set using a mean shift based clustering procedure. Positions on a smooth surface were found by moving every sample to maximum likelihood positions. Jenke *et al.*(2006) showed how to generate a smooth point cloud from a given noisy one using Bayesian statistics.

(4) Extension of 2D filters to 3D ones. The 2D filters were directly extended into 3D settings to smooth PSSs by applying local position estimating iteratively or non-iteratively, isotropically or anisotropically, based on statistics, differential geometry theory, approximation theory, etc.

The last group is more attractive since it is simple and straightforward. Techniques for image smoothing such as Laplacian, bilateral and trilateral filtering, moreover, commonly act as foundations for 3D surface denoising algorithms.

In this paper, we introduce a non-local denoising (NLD) method for PSSs inspired by a non-local algorithm for image denoising (Buades *et al.*, 2005) which presents remarkable results. Unlike the non-local image filter, our filter computes the denoised position of a vertex as a weighted average of the vertices in its vicinity with similar geometry features which are determined by mean shift clustering. The non-local approach defines the intensity similarity of two points by comparing regions of the surface around the vertices rather than using only their positions and sometimes normals locally. This yields a more accurate denoising result of the surface and improves the removal of higher-level noises compared to previous state-of-the- art filtering techniques. Moreover, fine geometry features are better preserved. An example of the effectiveness of our approach is presented in Fig.1. In this paper all the point models are rendered by using a point-based rendering technique.

The rest of this paper is organized as follows. In Section 2, we briefly review the related works. In Section 3, we briefly overview the non-local means approach of Buades, Coll, and Morel. We present our similarity-based method for denoising PSSs in Section 4. We compare our method with two denoising techniques in Section 5. Section 6 concludes the paper.

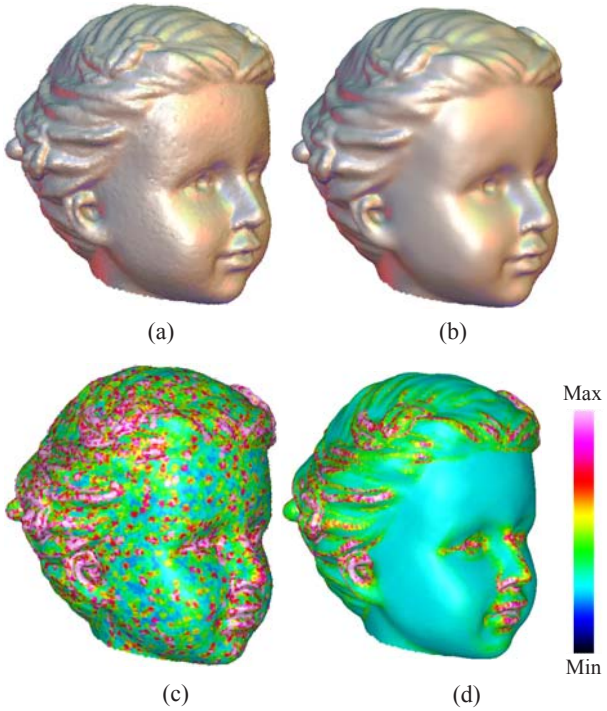

Fig.1 Denoising Buste model with our method. (a) Noisy model; (b) Model denoised by our method; (c) Noisy model colored by mean curvature; (d) Denoised model colored by mean curvature. Notice that high-frequency noise is properly removed, while fine details in hair region are accurately preserved

RELATED WORKS

Earlier methods such as Laplacian (Pauly *et al*., 2002b) for denoising PSSs are isotropic, which result commonly in point drifting and oversmoothing. So the anisotropic methods were introduced. Clarenz *et al*.(2004) presented a PDE-based surface fairing application within the framework of processing point-based surface via PDEs. Lange and Polthier (2005) proposed a new method for anisotropic fairing of a point-sampled surface based on the concept of anisotropic geometric mean curvature flow. Based on dynamic balanced flow, Xiao *et al*.(2006) presented a novel approach for fairing point-sampled geometry. Other methods have also been proposed for denoising the PSSs. Algorithms that recently attracted the interest of many researchers are MLS approaches. Based on MLS or its variants, the algorithms for denoising PSSs have also been introduced (Mederos *et al*., 2003; Weyrich *et al*., 2004; Dey and Sun, 2005;

Lipman *et al*., 2006; Daniels II *et al*., 2007). The main problem of MLS-based methods is that prominent shape features are blurred while smoothing PSSs. All of the above methods did not take into consideration the similarity of geometry features of sample points. Hu *et al*.(2006) introduced a mean shift based denoising algorithm for PSSs. During the course of denoising PSSs, they respected the kind of similarity via a 3D mean shift procedure. However, all the above-mentioned methods determine the intensity similarity of two points locally using only their positions and sometimes normals.

Concerning these issues, this paper defines the intensity similarity in a non-local fashion and takes into account the similarity of geometry features while denoising PSSs. We introduce the following techniques to achieve the non-local denoising algorithm: (1) By using the trilateral filtering operator, the geometry intensity of each sample point is determined; (2) Based on covariance analysis, a regular grid of geometry intensity is constructed for each point and the geometry-intensity similarity between two points is measured; (3) Based on mean shift clustering, the PSSs are clustered according to the surface-features similarity.

NON-LOCAL IMAGE DENOISING

The non-local algorithm for image denoising was proposed by Buades *et al*.(2005). The basic idea behind the non-local method is very simple: for a given pixel, its denoised intensity value is estimated as a weighted average of the other image pixels with weights reflecting the similarity between local neighborhoods of the pixel being processed and the other pixels.

More precisely, if an image $\Omega=\{I(\boldsymbol{u})|\boldsymbol{u}\in P\}$ is given, where $\boldsymbol{u}=(x, y)$ is a pixel and $I(\boldsymbol{u})$ is the intensity value at $\boldsymbol{u}$, the smoothed pixel intensity $I'(\boldsymbol{u})$ can be computed as the average of all pixel intensities in the image weighted by a similarity factor $\Phi(\boldsymbol{u},\boldsymbol{v})$,

$$I'(\boldsymbol{u})=\frac{\sum_{\boldsymbol{v}\in P}\Phi(\boldsymbol{u},\boldsymbol{v})I(\boldsymbol{v})}{\sum_{\boldsymbol{v}\in P}\Phi(\boldsymbol{u},\boldsymbol{v})}, \tag{1}$$

where $\Phi(\boldsymbol{u},\boldsymbol{v})=\exp(-S_{\boldsymbol{u},\boldsymbol{v}}/h^2)$. The parameter h acts as a degree of filtering, and the similarity $S_{\boldsymbol{u},\boldsymbol{v}}$ between $\boldsymbol{u}$ and $\boldsymbol{v}$ is measured as

$$S_{\boldsymbol{u},\boldsymbol{v}}=\sum_{\boldsymbol{o}}G_a(\|\boldsymbol{o}\|)\left|I(\boldsymbol{u}+\boldsymbol{o})-I(\boldsymbol{v}+\boldsymbol{o})\right|^2, \tag{2}$$

which depends on the pixel-wise intensity difference of two square neighborhoods centered at the pixels $\boldsymbol{u}$ and $\boldsymbol{v}$. The vector $\boldsymbol{o}$ denotes the offset between the center pixel and an arbitrary neighborhood pixel. The influence of a pixel pair on the similarity falls with increasing Euclidean distance to the center of the neighborhoods. For the distance weighting a Gaussian kernel $G_a(\cdot)$ with a standard deviation $a>0$ is used.

NON-LOCAL DENOISING ALGORITHM FOR PSSs

For the reason that image pixels are usually aligned on a regular and equispaced grid, which is in general not true for a point-sampled model, the main difficulty of extending the non-local method to PSSs consists of how to determine the intensity similarity of two points. Our strategy for solving this issue is as follows. By using the trilateral filtering operator, the differential value of each sample point is determined and called geometry intensity as a counterpart to the intensity value of an image. Based on covariance analysis, the local reference plane is defined on which a regular grid of geometry intensity is then constructed for each point, and according to geometry intensities on the corresponding grids, the geometry-intensity similarity of two points is finally measured.

Computation of geometry intensity

Although the trilateral filter presented by Choudhury and Tumblin (2003) for high contrast images and meshes can be extended to PSSs, it does not consider the curvature-related information. We design the following trilateral filter with the curvature-related term to compute the geometry intensity δ_i of each point $\boldsymbol{p}_i$

$$\begin{cases}\delta_i=\sum_{\boldsymbol{q}_{ij}\in N(\boldsymbol{p}_i)}w_{ij}<\boldsymbol{n}_i,\boldsymbol{q}_{ij}-\boldsymbol{p}_i>\Big/\sum_{\boldsymbol{q}_{ij}\in N(\boldsymbol{p}_i)}w_{ij},\\ w_{ij}=w_{\mathrm{c}}(\|\boldsymbol{q}_{ij}-\boldsymbol{p}_i\|)w_{\mathrm{s}}(\|<\boldsymbol{n}_i,\boldsymbol{q}_{ij}-\boldsymbol{p}_i>\|)w_{\mathrm{h}}(\|H_{ij}-H_i\|),\end{cases} \tag{3}$$

where $\boldsymbol{n}_i$ is the surface normal at the point $\boldsymbol{p}_i$, $N(\boldsymbol{p}_i)$ is the neighborhood of $\boldsymbol{p}_i$, H_i is the mean curvature and $w(\boldsymbol{x})$ is a Gaussian kernel: $w_{\mathrm{c}}(\boldsymbol{x})=\exp[-\boldsymbol{x}^2/(2\sigma_{\mathrm{c}}^2)]$,

$w_s(\boldsymbol{x})=\exp[-\boldsymbol{x}^2/(2\sigma_s^2)]$ and $w_h(\boldsymbol{x})=\exp[-\exp(-\|H_{ij}-H_i\|^2/2)]$. The term $w_h(\boldsymbol{x})$ denotes that the influence on the weight w_{ij} increases with an increase in the curvature difference $(H_{ij}-H_i)$ so that the high gradient regions can be efficiently smoothed. In this paper we take the parameter σ_c as $\sigma_c=r/2$, where r is the radius of the enclosing sphere of $N(\boldsymbol{p}_i)$, and σ_s as the standard deviation of the projections of the vector $(\boldsymbol{q}_{ij}-\boldsymbol{p}_i)$ onto $\boldsymbol{n}_i$.

Because our trilateral filtering operator considers not only the point positions and normals but curvatures, the geometry intensity computed by it can reflect the local geometry feature and describe the differential property at each point more efficiently. Fig.2b demonstrates the geometry-intensity value visualization of the points for the Face model. Fig.2e illustrates the palette for visualization of mean curvature, geometry intensity and the distance between two points.

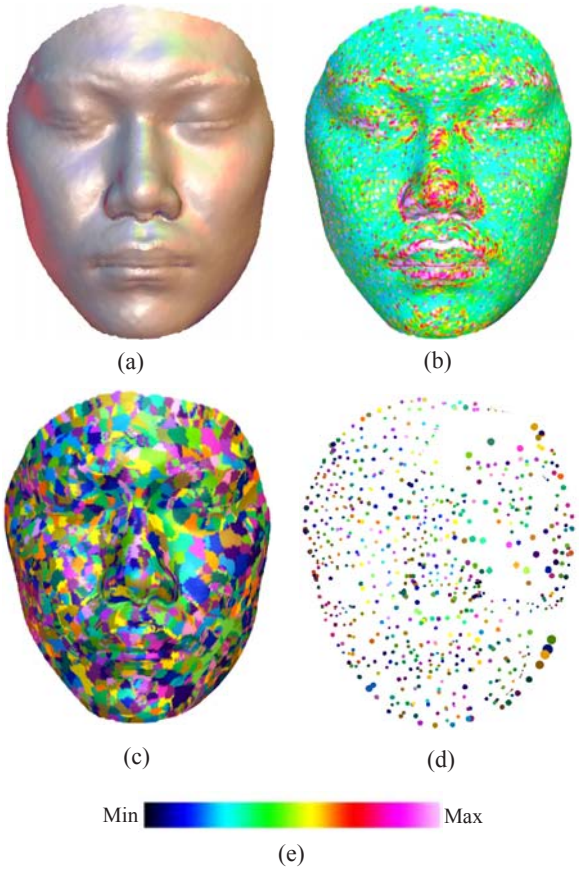

Fig.2 (a) Noisy Face model; (b) Geometry-intensity value visualization of the points; (c) Our mean-shift clustering; (d) The point set of local modes; (e) Palette for visualization of geometry intensity

Measuring the geometry-intensity similarity of two points

By covariance analysis, a local frame can be constructed based on the tangent plane and normal for each sample point. The covariance matrix for the point set P is defined as

$$\boldsymbol{C}=\begin{bmatrix}\boldsymbol{p}_{i_1}-\overline{\boldsymbol{p}}\\ \boldsymbol{p}_{i_2}-\overline{\boldsymbol{p}}\\ \vdots\\ \boldsymbol{p}_{i_k}-\overline{\boldsymbol{p}}\end{bmatrix}^{\mathrm{T}}\begin{bmatrix}\boldsymbol{p}_{i_1}-\overline{\boldsymbol{p}}\\ \boldsymbol{p}_{i_2}-\overline{\boldsymbol{p}}\\ \vdots\\ \boldsymbol{p}_{i_k}-\overline{\boldsymbol{p}}\end{bmatrix},$$

where $\boldsymbol{p}_{i_k}$ is the kth neighboring point around $\boldsymbol{p}_i$ and $\overline{\boldsymbol{p}}=\sum\boldsymbol{p}_{i_k}/k$ is the centroid of the neighborhood. Since $\boldsymbol{C}$ is symmetric and positive semi-definite, all eigenvalues λ_i (i=0, 1, 2) are of real value and the eigenvectors $\boldsymbol{v}_i$ (i=0, 1, 2) form an orthogonal basis. The eigenvalue λ_i measures the variation of the local point set along the direction of the corresponding eigenvector.

Assuming $\lambda_0\le\lambda_1\le\lambda_2$, let the plane $(\boldsymbol{x}-\overline{\boldsymbol{p}})\cdot\boldsymbol{v}_0=0$ through $\overline{\boldsymbol{p}}$ minimize the sum of the squared distance to the neighboring points of $\boldsymbol{p}_i$, then the normal $\boldsymbol{v}_0$ of this plane can be regarded as the normal of the local surface at $\boldsymbol{p}_i$. In this particular case, λ_0 expresses the variation of the surface along the normal $\boldsymbol{v}_0$. Pauly *et al.*(2002a) defined

$$\sigma_k^i=\sigma_k(\boldsymbol{p}_i)=\lambda_0/(\lambda_0+\lambda_1+\lambda_2) \tag{4}$$

as the surface variation at $\boldsymbol{p}_i$ assuming a neighborhood of size k. It is also observed that $\sigma_k(\boldsymbol{p}_i)$ is closely related to the local curvature. To ensure a consistent orientation of the normal vectors, we use a method based on the minimum spanning tree (Hoppe *et al.*, 1992).

For each point, we construct the local frame ($\boldsymbol{v}_2$, $\boldsymbol{v}_1$, $\boldsymbol{v}_0$) with the local origin $\boldsymbol{p}_i$ and on the plane $\boldsymbol{v}_2\boldsymbol{p}_i\boldsymbol{v}_1$, a regular geometry-intensity grid G_i with the size of $M\times M$ centered at $\boldsymbol{p}_i$ can be built by an interpolation method.

Let $N_R(\boldsymbol{p}_i)=\{\boldsymbol{q}_{ij}|\boldsymbol{q}_{ij}\in P_n,\ \|\boldsymbol{q}_{ij}-\boldsymbol{p}_i\|\le M|E|\}$ be the set of the neighbors of $\boldsymbol{p}_i$ whose elements are within a fixed radius R bound centered at $\boldsymbol{p}_i$, where $|E|=\sum_{i=0}^{n-1}r_{i\,\min}/n$ is the average edge length of the sample

point set P_n, $n=|P_n|$ and $r_{i\min}$ is the distance between $\boldsymbol{p}_i$ and its nearest point. Assuming that the vector $\boldsymbol{v}_g$ is the projection of the vector $(\boldsymbol{q}_{ij}-\boldsymbol{p}_i)$ onto the plane $\boldsymbol{v}_2\boldsymbol{p}_i\boldsymbol{v}_1$ and δ_g is the geometry intensity of the point $\boldsymbol{q}_{ij}$, the geometry intensity δ_m of each node $\boldsymbol{g}_m$ ($0\le m\le M\times M-1$) among G_i is estimated as

$$\delta_m=\frac{\sum_{\boldsymbol{v}_g\in N(\boldsymbol{g}_m)} w_g(\boldsymbol{v}_g)\delta_g}{\sum_{\boldsymbol{v}_g\in N(\boldsymbol{g}_m)} w_g(\boldsymbol{v}_g)},$$

where $N(\boldsymbol{g}_m)$ is the neighborhood of $\boldsymbol{g}_m$ and $w_g(\boldsymbol{x})$ is a Gaussian kernel: $w_g(\boldsymbol{v}_g)=\exp[-\|\boldsymbol{v}_g-\boldsymbol{g}_m\|^2/(2\sigma_g^2)]$. In this paper, we take again the parameter σ_g as $\sigma_g=r/2$, where r is the radius of the enclosing circle of $N(\boldsymbol{g}_m)$. When the regular geometry-intensity grid G_i of $\boldsymbol{p}_i$ is regarded as a counterpart to the square neighborhood of the pixel $\boldsymbol{u}$, we can, as a result, measure the geometry-intensity similarity of two points by means of Eq.(2).

Mean shift clustering for PSSs

Unlike the non-local image filtering algorithm, we do not sum over all point positions to filter a point but over a local neighborhood of this point which is determined by a mean shift clustering method. The mean shift algorithm is a nonparametric clustering technique for the analysis of a complex multimodal feature space and the delineation of arbitrarily shaped clusters (Comaniciu and Meer, 2002), and it has a wide variety of applications in the fields of computer vision and pattern recognition. Recently it has been extended to the field of digital geometry processing (Yamauchi *et al*., 2005; Hu *et al*., 2006; Shamir *et al*., 2006). In the following we first present a short review of the adaptive mean shift technique and then describe how to apply it to the point model.

Assume that each data point $\boldsymbol{x}_i\in\mathbb{R}^d$ ($i=1,2,\ldots,n$) is associated with a bandwidth value $h_i>0$. The sample point estimator (Georgescu *et al*., 2003; Yamauchi *et al*., 2005)

$$\hat{f}_K(\boldsymbol{x})=\frac{1}{nh_i^d}\sum_{i=1}^{n}K\left(\left\|(\boldsymbol{x}-\boldsymbol{x}_i)/h_i\right\|^2\right) \tag{5}$$

based on a spherically symmetric kernel K with bounded support satisfying

$$K(\boldsymbol{x})=c_{k,d}k(\|\boldsymbol{x}\|^2)>0,\quad \|\boldsymbol{x}\|\le 1$$

is an adaptive nonparametric estimator of the density at location $\boldsymbol{x}$ in the feature space. The function $k(\boldsymbol{x})$ ($0\le\boldsymbol{x}\le 1$) is called the profile of the kernel, and the normalization constant $c_{k,d}$ assures that $K(\boldsymbol{x})$ integrates to one. The function $g(\boldsymbol{x})=-k'(\boldsymbol{x})$ can always be defined when the derivative of the kernel profile $k(\boldsymbol{x})$ exists. Using $g(\boldsymbol{x})$ as the profile, the kernel $G(\boldsymbol{x})$ is defined as $G(\boldsymbol{x})=c_{g,d}g(\|\boldsymbol{x}\|^2)$.

By taking the gradient of Eq.(5) the following property can be proven

$$\boldsymbol{m}_G(\boldsymbol{x})=C\hat{\nabla}f_K(\boldsymbol{x})\big/\hat{f}_G(\boldsymbol{x}),$$

where C is a positive constant and

$$\boldsymbol{m}_G(\boldsymbol{x})=\frac{\sum_{i=1}^{n}\frac{\boldsymbol{x}_i}{h_i^{d+2}}g\left(\left\|(\boldsymbol{x}-\boldsymbol{x}_i)/h_i\right\|^2\right)}{\sum_{i=1}^{n}\frac{1}{h_i^{d+2}}g\left(\left\|(\boldsymbol{x}-\boldsymbol{x}_i)/h_i\right\|^2\right)}-\boldsymbol{x} \tag{6}$$

is called the mean shift vector pointing toward the direction of the maximum increase in the density. A gradient-ascent process with an adaptive step size

$$\boldsymbol{y}^{[j+1]}=\boldsymbol{m}_G(\boldsymbol{y}^{[j]}),\quad j=0,1,2,\ldots \tag{7}$$

constitutes the core of the mean shift clustering procedure. For clustering $S=\{\boldsymbol{x}_1,\boldsymbol{x}_2,\ldots,\boldsymbol{x}_n\}$ with mean shift, the following two steps are performed on each $\boldsymbol{x}_i\in S$: (1) Initialize $\boldsymbol{y}_i^{[0]}$ with $\boldsymbol{x}_i$; (2) Compute $\boldsymbol{y}_i^{[j]}$ according to Eq.(7) until convergence. It is shown in (Comaniciu and Meer, 2002) that under some general assumptions the sequences $\{\boldsymbol{y}_i^{[j]}\}$ converge to the points where $\hat{f}_K(\boldsymbol{x})$ defined by Eq.(5) attains its local maxima (mode). Accordingly, the points that converge to the same mode are associated with the same cluster.

One simple extension of the above clustering procedure consists of dealing with a set S, each element of which has two components of a different nature, $S=\{\boldsymbol{x}_i=(\boldsymbol{c}_i,\boldsymbol{q}_i)|\boldsymbol{c}_i\in C,\boldsymbol{q}_i\in Q\}$. In such a situation, it is convenient to use the mean shift clustering procedure with separable kernels

$$\hat{f}_K(\boldsymbol{x})=\frac{1}{nh_{i_1}^{d_1}h_{i_2}^{d_2}}\sum_{i=1}^{n}k_1\left(\left\|(\boldsymbol{c}-\boldsymbol{c}_i)/h_{i_1}\right\|^2\right)k_2\left(\left\|(\boldsymbol{q}-\boldsymbol{q}_i)/h_{i_2}\right\|^2\right).$$

In this paper, we consider the sample points $\{\boldsymbol{p}_i\}$ equipped with the normals $\{\boldsymbol{n}_i\}$ and the mean curvature $\{H_i\}$ as scattered data $S=\{\boldsymbol{x}_i=(\boldsymbol{c}_i,\boldsymbol{q}_i)|\boldsymbol{c}_i\in\boldsymbol{p}_i, \boldsymbol{q}_i\in(\boldsymbol{n}_i, H_i)\}$ in $\mathbb{R}^7$. For both $\boldsymbol{c}_i$ and $\boldsymbol{q}_i$, we use the normal kernel. For the bandwidth values h_i, there are numerous methods to define them, most of which use a pilot density estimate. The simplest way to obtain the pilot density estimate is by nearest neighbors. To accelerate the mean shift computation, we construct a k-D tree for the point set $\{\boldsymbol{c}_i\}$. According to the k-nearest neighbors $N_k(\boldsymbol{c}_i)$ of $\boldsymbol{c}_i$, we can adaptively take $h_{i_1}=\|\boldsymbol{c}_i-\boldsymbol{c}_{i,k}\|_2$, where $\boldsymbol{c}_{i,k}$ is the k-nearest neighbor of $\boldsymbol{c}_i$, and $h_{i_2}=\max\{\|\boldsymbol{q}_i-\boldsymbol{q}_{i,1}\|_2, \|\boldsymbol{q}_i-\boldsymbol{q}_{i,2}\|_2, \ldots, \|\boldsymbol{q}_i-\boldsymbol{q}_{i,k}\|_2\}$. After clustering for PSSs by using this mean shift technique, the geometry features of the points in the same cluster, which contain the point positions, normals and mean curvatures, are locally similar, respectively. Fig.2c demonstrates the mean shift clustering of the Face model, and its point set of local modes is illustrated in Fig.2d.

Non-local denoising of PSSs

From the geometry-intensity similarities of two points and Eq.(1), we can compute the denoised geometry intensity δ_i' of $\boldsymbol{p}_i$ as

$$\delta_i'=\sum_{\boldsymbol{q}_{ij}\in C(\boldsymbol{p}_i)}\left(\Phi(\boldsymbol{p}_i,\boldsymbol{q}_{ij})\delta_{ij}\right)\Big/\sum_{\boldsymbol{q}_{ij}\in C(\boldsymbol{p}_i)}\Phi(\boldsymbol{p}_i,\boldsymbol{q}_{ij}),$$

where $C(\boldsymbol{p}_i)$ is the cluster to which $\boldsymbol{p}_i$ belongs, i.e., a local neighborhood of $\boldsymbol{p}_i$ determined by our mean shift clustering method. The similarity factor $\Phi(\boldsymbol{p}_i, \boldsymbol{q}_{ij})$ is computed by

$$\Phi(\boldsymbol{p}_i,\boldsymbol{q}_{ij})=\exp(-S_{\boldsymbol{p}_i,\boldsymbol{q}_{ij}}/h^2),$$

where the geometry-intensity similarity $S_{\boldsymbol{p}_i,\boldsymbol{q}_{ij}}$ between $\boldsymbol{p}_i$ and $\boldsymbol{q}_{ij}$ is measured by the method described in the subsection "Measuring the geometry-intensity similarity of two points".

According to the offset distance δ_i', the smoothed position $\boldsymbol{p}_i'$ is given by $\boldsymbol{p}_i'=\boldsymbol{p}_i+\delta_i'\boldsymbol{n}_i$. Since the point $\boldsymbol{p}_i$ is moved along its normal direction, our denoised method will not introduce undesirable points drifting over the surface. Moreover, this method is more effective and robust than the local denoising methods as it considers not only the geometry-features similarity between two points but also the geometry-intensity similarity between them.

RESULTS AND DISCUSSION

In our experiments, we use Microsoft Visual C++ programming language on a personal computer with a Pentium IV 2.8 GHz CPU and 1 GB main memory. We have implemented our non-local denoising (NLD) and two state-of-the-art denoising techniques: the Bilateral denoising (BIL) (Fleishman *et al.*, 2003) and the Mean Shift denoising (MST) (Hu *et al.*, 2006) to compare their denoising results. We use three models in our comparison: a noisy Buste model with 125 813 sample points (Fig.1a), a noisy Face model with 34 308 sample points (Fig.2a) and a noisy Dragon-head model with 100 056 sample points (Fig.3). For these models, Table 1 presents the related statistics and parameter settings used for our method and our implementations of BIL and MST. For BIL and MST, we tried to choose the parameter settings that produce the best results.

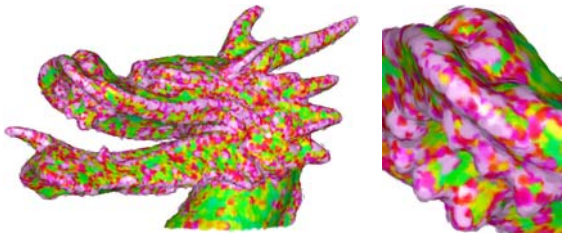

(a) (b)

Fig.3 (a) Noisy Dragon-head model colored by mean curvature; (b) Closer view of its upper jaw

Table 1 Parameter setting and the related statistics

Fig.	Method	Iters.	Sim.	k	Max. error ($\times10^{-4}$)	Avg. error ($\times10^{-4}$)	T_{MS} (s)	T_D (s)
4	BIL	1	–	15	89.3	4.5	–	2.77
	MST	1	–	15	51.9	3.3	15.1	3.52
	NLD	1	5×5	15	31.3	2.4	15.1	15.31
5	BIL	2	–	20	78.0	15.3	–	7.56
	MST	3	–	20	75.3	14.8	72.4	13.32
	NLD	3	9×9	20	68.9	14.1	72.4	109.92
6	BIL	3	–	23	131.7	19.5	–	9.03
	MST	3	–	23	96.5	16.8	98.7	14.02
	NLD	3	9×9	23	74.2	13.3	98.7	148.58

Iters. stands for the number of iterations. Sim. is the size of the regular grid considered to measure the geometry-intensity similarity of two points. For BIL, k is the number of the neighbors, and for NLD and MST, k is the number of the sample points in bandwidth window for mean shift clustering. Max. error is the maximum of distances between the original (noisy) points and their corresponding denoised points, and Avg. error is the average of distances. T_{MS} indicates the time of implementing the mean shift clustering and T_D denotes the point estimating time for one iteration

We use two visualization schemes to compare the techniques with our method. The first scheme consists of coloring by the mean curvature. The second one measures the difference between the original and denoised point model, i.e., we visualize the differences in the positions of the corresponding sample points of the models $|\boldsymbol{p}_i^{\text{noisy}} - \boldsymbol{p}_i^{\text{denoised}}|$.

In Fig.4, we demonstrate a comparison of the denoised Face models by BIL, MST and NLD. The denoised models are illustrated in the top row of Fig.4, and their corresponding mean curvature visualizations in the bottom row. As seen in Fig.4, our NLD removes the high-frequency noise properly and achieves a more accurate result than BIL or MST does. Fig.5 shows a comparison of BIL, MST and NLD concerning feature preservation. Note that our NLD preserves sharp features more accurately than BIL or MST does while producing a smooth result, as shown in the closer views of the upper jaw of the denoised model.

In Fig.1, we show the denoising efficiency of our approach on the noisy Buste model (Fig.1a), which is produced by adding zero-mean Gaussian noise with $\sigma_{\text{noise}}=0.3|E|$ to the original model. It can be noticed that the high-frequency noise is properly removed, while fine details in hair, mouth and ear regions are accurately preserved. At the same time, we demonstrate that our NLD presents the best performance according to the entropy of the differences between the noisy and denoised models, as shown in the bottom row of Fig.6. From the Max. and Avg. errors in Table 1 we can also notice that our method outperforms its two rivals. As a result, our method produces the lowest oversmoothing when compared with the other two denoising techniques.

Due to our region-based definition of the geometry-intensity similarity measure which adds more geometric information into the denoising process, our algorithm removes the high-frequency noise properly and achieves a more accurate result than BIL or MST does. Furthermore, our method has a better feature preservation than BIL or MST does while producing a smooth result, mainly because the method utilizes the trilateral filter in the denoising process. From the execution time listed in Table 1, we notice that our method is slower than BIL or MST since our method needs to construct the regular geometry-intensity grid for each sample point and measure the geometry-intensity similarity of two points.

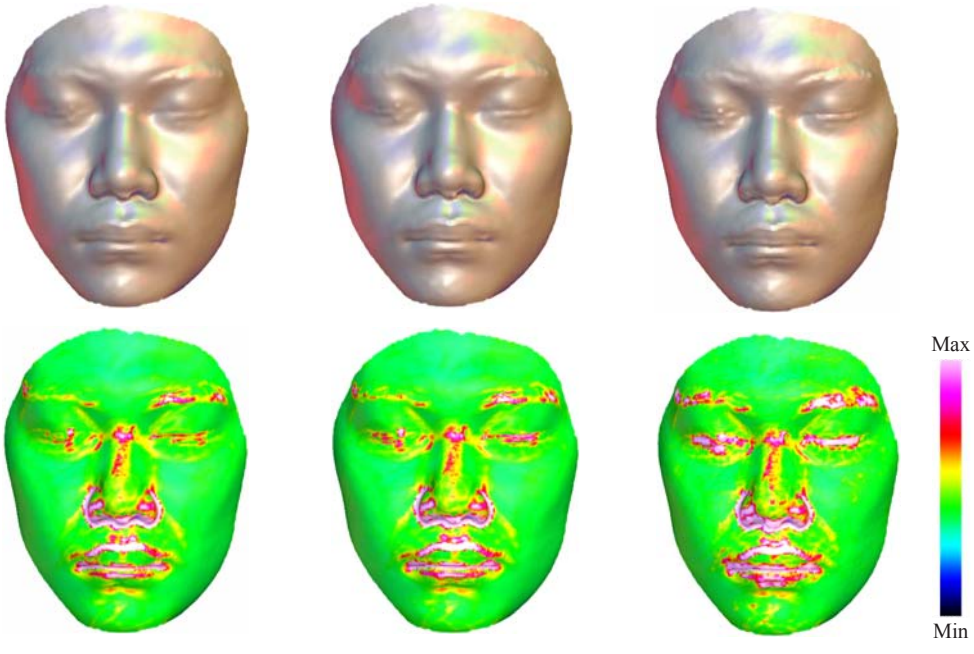

Fig.4 Denoising the noisy Face model (Fig.2a). Top: the denoised models. Bottom: the corresponding denoised model colored by mean curvature. Mean curvature coloring helps us to compare their corresponding fine details. (a) BIL; (b) MST; (c) NLD

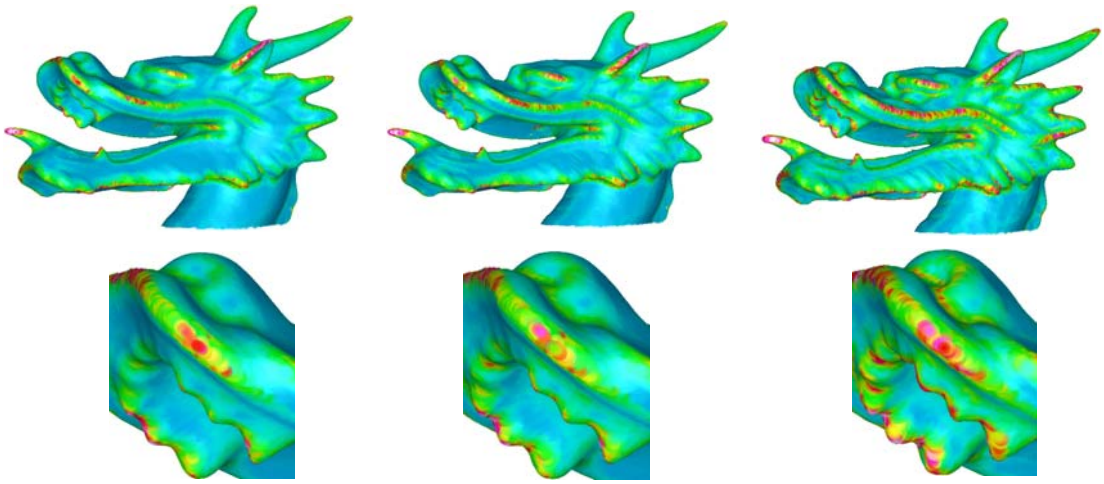

(a) (b) (c)

Fig.5 Denoising the noisy Dragon-head model (Fig.3). Top: the denoised model colored by mean curvature. Bottom: a closer view of the upper jaw of the corresponding denoised model. (a) BIL; (b) MST; (c) NLD

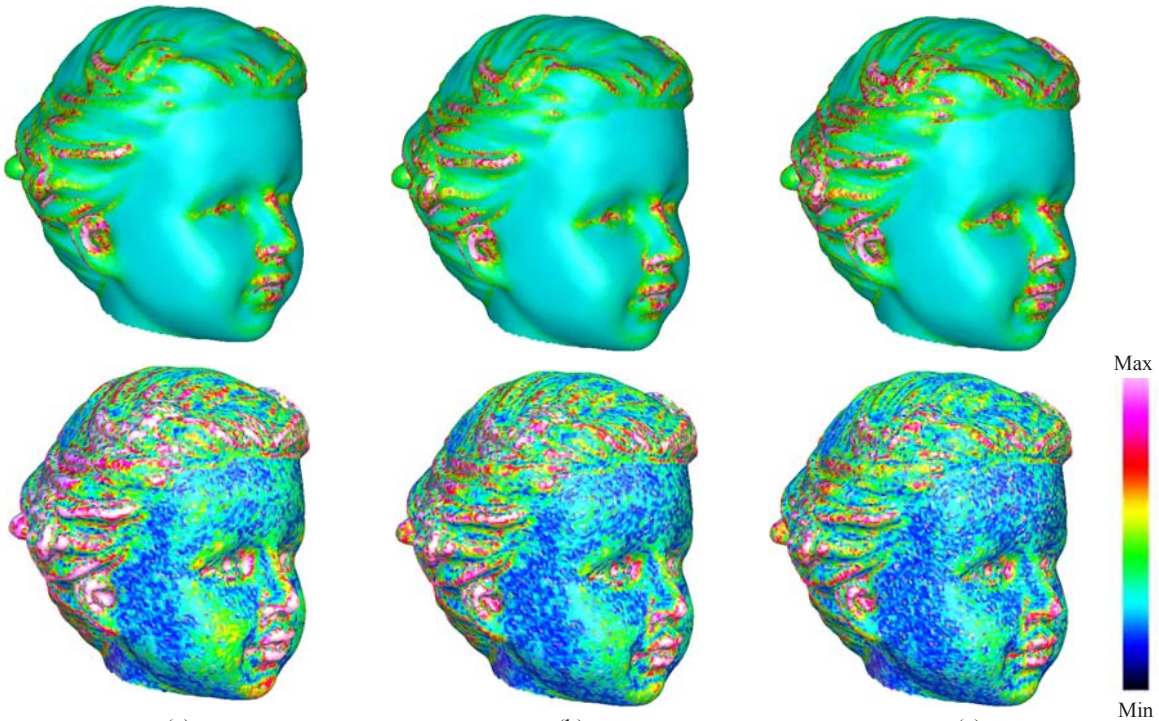

(a) (b) (c)

Fig.6 Denoising the noisy Buste model (Fig.1a). Top: the denoised model colored by mean curvature. Bottom: the corresponding denoised model colored according to the entropy of the differences between the noisy and denoised models. (a) BIL; (b) MST; (c) NLD

CONCLUSION

In this paper, we presented an NLD algorithm for PSSs by extending the non-local technique for image denoising to a point-sampled model. Since the original non-local method relies heavily on the image structure regularity, the main difficulty in extending it to PSSs is how to determine the intensity similarity of two sample points. We first compute the geometry intensity of the sample point by using the trilateral filtering operator. Based on covariance analysis, a regular geometry-intensity grid as a counterpart to the

square neighborhood of the pixel is then constructed. Finally, the geometry-intensity similarity of two points is measured according to their grids. Furthermore, the neighborhood of the sample point is adaptively selected in the denoising process by means of our mean shift method so as to produce a more accurate denoising result.

Our experimental results demonstrate that this proposed algorithm is robust, and can produce more accurate denoising results than the two state-of-the-art smoothing techniques, the Bilateral denoising and the Mean Shift denoising, while having better feature preservation.

ACKNOWLEDGEMENTS

Models are courtesy of Yutake Ohtake (Noisy Face), Thouis Jones (Noisy Dragon Head) and EU AIM@Shape project (Buste).

References

Amenta, N., Kil, Y.J., 2004. Defining point set surfaces. *ACM Trans. on Graph.*, **23**(3):264-270. [doi:10.1145/1015706.1015713]

Buades, A., Coll, B., Morel, J.M., 2005. A Non-Local Algorithm for Image Denoising. Proc. IEEE Computer Society Int. Conf. on Computer Vision and Pattern Recognition, p.60-65. [doi:10.1109/CVPR.2005.38]

Carr, J.C., Beatson, R.K., Cherrie, J.B., Mitchell, T.J., Fright, W.R., McCallum, B.C., Evans, T.R., 2001. Reconstruction and Representation of 3D Objects with Radial Basis Functions. Proc. ACM SIGGRAPH, p.67-76. [doi:10.1145/383259.383266]

Choudhury, P., Tumblin, J., 2003. The Trilateral Filter for High Contrast Images and Meshes. Int. Conf. on Computer Graphics and Interactive Techniques, p.186-196. [doi:10.1145/1198555.1198565]

Clarenz, U., Rumpf, M., Telea, A., 2004. Fairing of Point Based Surfaces. Proc. Computer Graphics International, p.600-603. [doi:10.1109/CGI.2004.1309272]

Comaniciu, D., Meer, P., 2002. Mean shift: a robust approach toward feature space analysis. *IEEE Trans. on Pattern Anal. Machine Intell.*, **24**(5):603-619. [doi:10.1109/34.1000236]

Daniels II, J., Ha, L.K., Ochotta, T., Silva, C.T., 2007. Robust Smooth Feature Extraction from Point Clouds. Proc. Shape Modeling International, p.123-136. [doi:10.1109/SMI.2007.32]

Dey, T.K., Sun, J., 2005. An Adaptive MLS Surface for Reconstruction with Guarantees. Proc. Symp. on Geometry Processing, p.43-52.

Fleishman, S., Drori, I., Cohen-Or, D., 2003. Bilateral mesh denoising. *ACM Trans. on Graph.*, **22**(3):950-953. [doi:10.1145/882262.882368]

Georgescu, B., Shimshoni, I., Meer, P., 2003. Mean Shift Based Clustering in High Dimensions: A Texture Classification Example. ICCV, p.456-463.

Hoppe, H., DeRose, T., Duchamp, T., McDonald, J., Stuetzle, W., 1992. Surface Reconstruction from Unorganized Points. Proc. 19th Annual Conf. on Computer Graphics and Interactive Techniques, p.71-78. [doi:10.1145/133994.134011]

Hu, G.F., Peng, Q.S., Forrest, A.R., 2006. Mean shift denoising of point-sampled surfaces. *The Visual Computer*, **22**(3):147-157. [doi:10.1007/s00371-006-0372-0]

Jenke, P., Wand, M., Bokeloh, M., Schilling, A., Strasser, W., 2006. Bayesian point cloud reconstruction. *Computer Graphics Forum*, **25**(3):379-388. [doi:10.1111/j.1467-8659.2006.00957.x]

Lange, C., Polthier, K., 2005. Anisotropic smoothing of point sets. *Computer Aided Geometric Design*, **22**(7):680-692. [doi:10.1016/j.cagd.2005.06.010]

Lipman, Y., Cohen-Or, D., Levin, D., 2006. Error Bounds and Optimal Neighborhoods for MLS Approximation. Proc. Eurographics, p.71-80. [doi:10.2312/SGP/SGP06/071-080]

Mederos, B., Velho, L., de Figueiredo, L.H., 2003. Robust Smoothing of Noisy Point Clouds. Proc. SIAM Conf. on Geometric Design and Computing, p.1-13.

Pauly, M., Gross, M., 2001. Spectral Processing of Point-Sampled Geometry. Proc. ACM SIGGRAPH, p.379-386. [doi:10.1145/383259.383301]

Pauly, M., Gross, M., Kobbelt, L.P., 2002a. Efficient Simplification of Point-Sampled Surfaces. Proc. IEEE Visualization, p.163-170.

Pauly, M., Kobbelt, L.P., Gross, M., 2002b. Multiresolution Modeling of Point-Sampled Geometry. Technical Report, CS #379, ETH, Zurich.

Pauly, M., Keiser, R., Kobblet, L.P., Gross, M., 2003. Shape modeling with point-sampled geometry. *ACM Trans. on Graph.*, **22**(3):641-650. [doi:10.1145/882262.882319]

Pauly, M., Mitra, N.J., Guibas, L.J., 2004. Uncertainty and Variability in Point Cloud Surface Data. Proc. Eurographics Symp. on Point-Based Graphics, p.77-84.

Samozino, M., Alexa, M., Alliez, P., Yvinec, M., 2006. Reconstruction with Voronoi Centered Radial Basis Functions. Proc. Eurographics, p.51-60. [doi:10.2312/SGP/SGP06/051-060]

Schall, O., Belyaev, A., Seidel, H.P., 2005. Robust Filtering of Noisy Scattered Point Data. Eurographics Symp. on Point-Based Graphics, p.71-77. [doi:10.2312/SPBG/SPBG05/071-077]

Shamir, A., Shapira, L., Cohen-Or, D., 2006. Mesh analysis using geodesic mean-shift. *The Visual Computer*, **22**(2):99-108. [doi:10.1007/s00371-006-0370-2]

Weyrich, T., Pauly, M., Keiser, R., Heinzle, S., Scandella, S., Gross, M., 2004. Post-processing of Scanned 3D Surface Data. Proc. Eurographics, p.85-94.

Xiao, C.X., Miao, Y.W., Liu, S., Peng, Q.S., 2006. A dynamic balanced flow for filtering point-sampled geometry. *The Visual Computer*, **22**(3):210-219. [doi:10.1007/s00371-006-0377-8]

Yamauchi, H., Lee, S., Lee, Y., Ohtake, Y., Belyaev, A., Seidel, H.P., 2005. Feature Sensitive Mesh Segmentation with Mean Shift. Proc. Shape Modeling International, p.236-243. [doi:10.1109/SMI.2005.21]